CHAPTER 9

Detecting Changes in Forest Condition at Landscape Scales Using a Landsat-Based Harmonic Modeling Approach

Valerie J. Pasquarella,
Randall S. Morin,
Andrew M. Liebhold,
Nathan W. Siegert,
Clare A. Rodenberg,
and Kyle J. Haynes

How to cite this chapter:

Pasquarella, Valerie J.; Morin, Randall S.; Liebhold, Andrew M.; Siegert, Nathan W.; Rodenberg, Clare A.; Haynes, Kyle J. 2023. Detecting changes in forest condition at landscape scales using a Landsat-based harmonic modeling approach. In: Potter, Kevin M.; Conkling, Barbara L., eds. Forest Health Monitoring: national status, trends, and analysis 2022. Gen. Tech. Rep. SRS-273. Asheville, NC: U.S. Department of Agriculture, Forest Service, Southern Research Station: 149–162. https://doi.org/10.2737/SRS-GTR-273-Chap9.

INTRODUCTION

The health and condition of forested ecosystems are increasingly affected by a variety of disturbances including forest harvests, fires, and pests and pathogens (Cohen and others 2016, Lovett and others 2006). The Insect and Disease Survey (IDS), coordinated by the U.S. Department of Agriculture, Forest Service, Forest Health Protection, has historically used annual aerial surveys to map and monitor pest damage (Coleman and others 2018). However, remote sensing instruments are uniquely poised to provide consistent, regularly updated monitoring over large areas, and numerous forest disturbance detection and condition monitoring approaches have been developed (Cohen and others 2017, Hall and others 2007, Koltunov and others 2020, Rullan-Silva and others 2013, Senf and others 2017). These automated approaches can be combined with field datasets including systematic plot measurements from the Forest Service's Forest Inventory and Analysis (FIA) program to build an improved understanding of how the spatial and temporal distribution of disturbances affects forest structure, composition, and resilience (Lister and others 2020, Schroeder and others 2014, Vogt and Koch 2016). Yet monitoring short-duration changes, such as those associated with defoliating insect outbreaks, and characterizing the longer term effects of defoliator outbreaks remain an ongoing challenge.

Detecting changes in forest health and condition requires a formally designed baseline against which comparisons can be made (Norman and Christie 2020). In the context of spectral measurements, baselines are typically defined in terms of seasonally similar values from different years or other aggregate statistics (e.g., Chastain and others 2015, Norman and others 2013), but comparing individual observations from different years and/or times of year can be problematic due to potential differences in foliar phenology and other confounding factors, such as missed clouds and shadows and other uncorrected atmospheric effects. Given that forest ecosystems tend to have relatively stable and persistent phenological signals (Pasquarella and others 2016), cyclic patterns in the reflectance of forest ecosystems are typically well represented by regression models with harmonic terms that characterize seasonal variability while remaining robust to noisy observations (Wilson 2015; Wilson and others 2012, 2018; Zhu and others 2012). Thus, a harmonic baseline monitoring approach enables more direct comparison of observed and predicted values for specific dates.

Previous efforts to map the 2016–2018 forest defoliation caused by outbreak populations of the spongy moth (*Lymantria dispar*) in southern New England using a Landsat-based harmonic monitoring approach (Pasquarella and others 2017, 2018) relied on a single harmonic model to represent long periods of relative stability as a baseline for comparison. Although this fixed-baseline approach facilitated pre- and post-outbreak comparisons, the designated baseline period was highly dependent on the specific study area and disturbance of interest, and we found notable variations in the magnitude of disturbance for vegetation condition scores calculated using different baseline years (Pasquarella and others

2021). The fixed-baseline approach also posed a challenge in terms of generating historic assessments (since baseline fitting might overlap with monitoring dates) as well as when the baseline period is increasingly far into the past relative to the period being monitored (since the baseline becomes less representative of current conditions as time since fitting increases).

As a key deliverable of our Evaluation Monitoring project, we introduce a more flexible moving-window approach for Landsat-based harmonic condition monitoring (HCM) that considers both spatial and temporal variability in forest disturbance dynamics and improves our ability to estimate uncertainties in both near-real-time and aggregated seasonal assessments. In this summary, we briefly describe our method and efforts to operationalize our workflow for the northern portion of Forest Service Region 9 (Eastern Region) using the Google Earth Engine platform. We compare results generated using the new moving-window workflow with comparable fixed-baseline results for a set of field sites in central Massachusetts. We then tested the utility of HCM-generated vegetation condition scores for assessing relationships between defoliation and growth and mortality rates of oaks (*Quercus* spp.) in Pennsylvania using FIA plot measurements, building on previous work by Morin and Liebhold (2016) that relied on aerial survey data.

METHODS

Our HCM approach is based on the assumption that univariate time series of reflectance observations for a band or index of interest can be relatively well characterized by a harmonic regression model (Sellers and others 1996). This approach is particularly suited for condition monitoring using vegetation indices in regions/ecosystems with strong phenological signals. Although our methods could be adapted to other sensors, we currently rely on Landsat time series due to the length of the Landsat observation record (1985 to present) as well as moderate spatial (30-m) and temporal (8- to 16-day) resolutions. We use the following model to estimate baseline reflectance:

$$y(\mathrm{x}) = \mathrm{a} + bx + \sum_{j \in N} \left(\mathrm{c}_j \cos\left(\frac{2\pi j}{T}\mathrm{x}\right) + d_j \sin\left(\frac{2\pi j}{T}\mathrm{x}\right) \right) + \varepsilon$$

where

y = the predicted vegetation index, e.g., Tasseled Cap Greenness (TCG) (Crist 1985; Crist and Kauth 1986)

x = the ordinal date of each observation

a = the modeled intercept

b = the modeled slope

N = a set of integers specifying the frequency, j, of the Fourier series harmonics (e.g., $N = \{1, 3\}$, corresponding to 12-month and 4-month harmonics)

c_j = the cosine coefficients

d_j = the sine coefficients estimated at each frequency

T = the number of days in a year (T = 365.25)

ε = the residual error term for each observation

The use of a 4-month harmonic was preferred over a 6-month harmonic to characterize higher frequency asymmetry in the seasonal reflectance profile without adding an additional set of harmonic terms.

Once baseline reflectance models have been estimated, vegetation condition scores are calculated as the difference between the observed and predicted reflectance values for a given acquisition date, and are normalized by the root mean square error (RMSE) of the baseline model used to generate the predicted value, i.e.:

$$\text{score} = \frac{y - y_{pred}}{RMSE}$$

Thus, vegetation condition scores are a normalized anomaly metric that estimates the magnitude of change in reflectance relative to the uncertainty in baseline model fit.

Previous implementations of our HCM workflow that relied on a single baseline model for prediction and monitoring calculated a single vegetation condition score for each acquisition date during a specified monitoring period. However, selection of a suitable baseline period may be challenging in frequently disturbed landscapes. Furthermore, noise in reflectance observations may impact the quality of models fit to different time periods. Therefore, the latest version of our workflow utilizes an ensemble approach that combines vegetation condition score estimates from multiple baseline models (see Pasquarella 2021 for code). Baseline models are fit to Landsat time series using a moving window such that each model is fit to a unique time period in 1-year increments and the n models preceding the specified monitoring period are used to generate a set of n vegetation condition score estimates for each acquired image during the specified monitoring period. These scores can then be averaged across all dates within the monitoring period to produce a more robust estimate of potential condition change for each pixel in the specified study area. Although baseline length (in years) is an adjustable parameter in our workflow, we use a baseline period of 5 years (e.g., models are generated for 1985–1989, 1986–1990, 1987–1991, and so on), which provides a sufficient number of observations for fitting a six-term harmonic model while remaining responsive to temporally localized changes in reflectance patterns and approximating the FIA remeasurement cycle.

RESULTS AND DISCUSSION

Condition Monitoring Workflow and Visualization Tools

To demonstrate our ability to monitor changes in vegetation condition over large spatial extents, we piloted our improved HCM workflow for nine States in the northern portion of Forest Service Region 9, specifically Maine, New Hampshire, Vermont, New York, Massachusetts, Connecticut, Rhode Island, New Jersey, and Pennsylvania. We used time series of Landsat 5, 7, and 8 observations to generate annual maps of condition change assessments for the years 1995 to present using a May 1 through September 30 monitoring period. We applied the TCG coefficients for surface reflectance data (Crist 1985, Crist and Kauth 1986) to observations from all three Landsat sensors, assuming that observations are relatively well calibrated across sensors with any differences characterized in the error term. We selected the monitoring period to generally characterize vegetation change during the Northern Hemisphere growing season including spongy moth defoliation, which typically peaks in June. The monitoring period, however, is a user-specified input in our workflow and can range from single-date predictions, which provide the most precise estimates of timing but may include gaps due to masking cloud and shadow artifacts, to longer monitoring periods that average over multiple observations to provide more robust estimates and improve spatial coverage. Our final assessment products combine results across Landsat orbital paths and include per-pixel mean and standard deviation of scores, mean and standard deviation of observed TCG, and number of observations. The use of multiple shorter baselines eliminates the need to specify a single longer baseline *a priori* and enables characterization of uncertainty in condition score across models.

We developed a Condition Monitoring Explorer application (app) to facilitate interactive exploration of annual results. The tool displays a series of annual vegetation condition assessment maps as well as time series of results for clicked points (fig. 9.1). Pre-cached results for more than 2 decades load quickly, and condition change patterns can be compared through time at a variety of spatial extents and using different disturbance severity thresholds. The app along with its code and workflow are publicly available (Pasquarella 2021) and can be updated, extended, and modified as needed. Users can also request access to baseline model and condition assessment assets, which are updated periodically to reflect changes in Landsat collections and other processing improvements.

The mapped results characterize expected patterns, such as severe defoliation by spongy moth across Rhode Island and eastern Connecticut in 2016 (fig. 9.1). Because the approach is currently based purely on spectral change, we also detect TCG anomalies associated with other types of change, such as human development (e.g., vegetation clearing for construction) and extreme weather events like the 2011 tornado in Springfield, MA. Given that the series of baseline models are fit to observations from years immediately preceding the target monitoring year, some baseline periods for sites experiencing multiyear disturbances will include years with decreased TCG. When vegetation does not recover, i.e., in the case of permanent clearing or development, we would expect baselines to adjust to the new normal, with vegetation condition scores returning to near-zero values. In cases where post-disturbance regrowth or other increases in vegetation cover and vigor are observed, we expect to see positive anomalies, i.e., above-baseline TCG values, indicating that TCG in the monitoring year is higher than the predicted values estimated from baselines including disturbed states.

Comparisons with Previous Implementations

The HCM workflow was initially developed to characterize defoliation events, and assessments generated using fixed-baseline versions have been

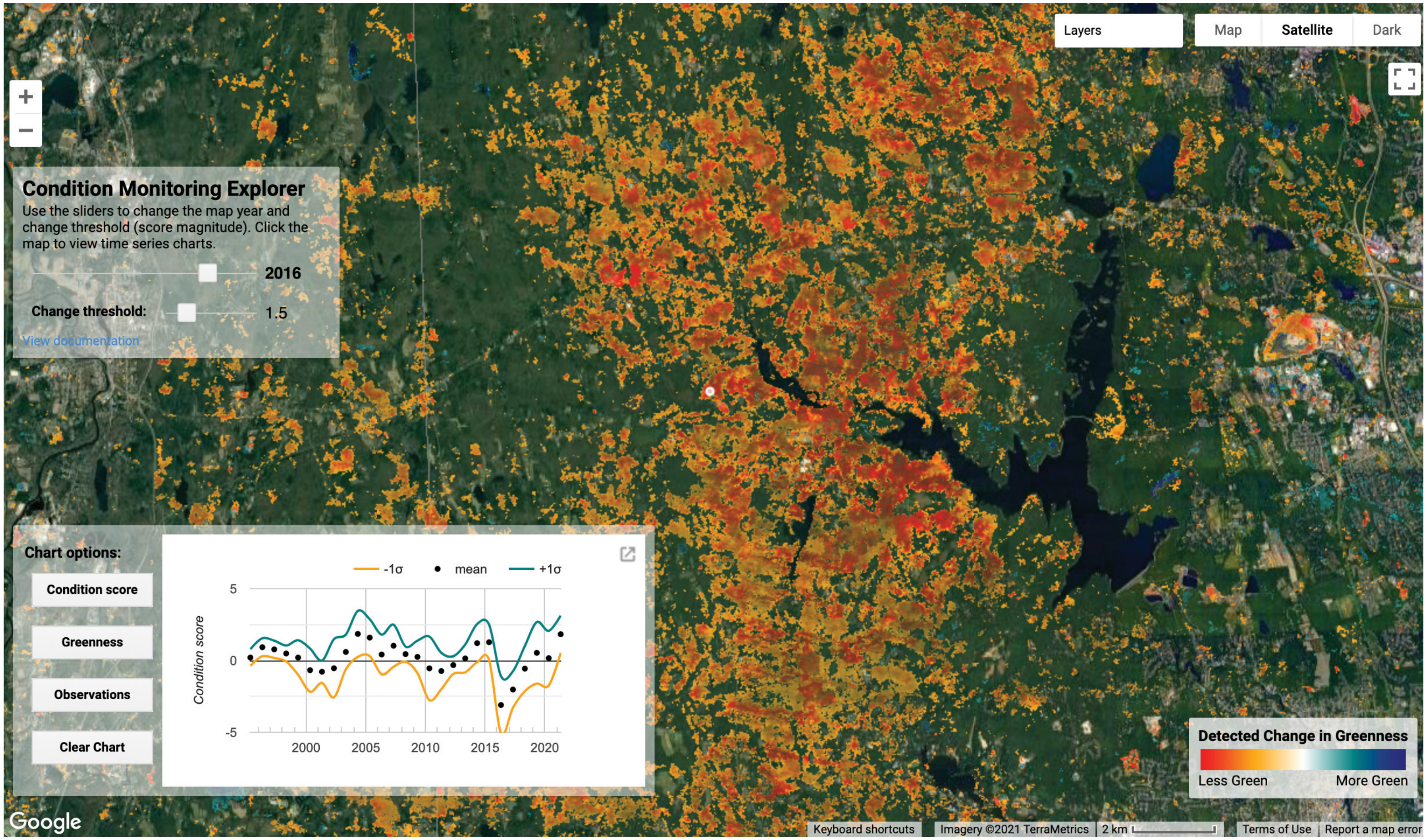

Figure 9.1—Severe defoliation by spongy moth across Rhode Island and eastern Connecticut in 2016 as seen in the Condition Monitoring Explorer app in Google Earth Engine (https://valeriepasquarella.users.earthengine.app/view/condition-monitoring-explorer). This tool allows users to visualize annual condition change estimates for 1995 to present. Adjusting the year slider changes the map year displayed, and the change threshold slider adjusts a mask on the magnitude of change ranging from 0 (all changes) to 4 (four or more times the estimated baseline root mean square error). Clicking a point on the mapped area displays time series of condition scores, Tasseled Cap Greenness, and number of observations for the corresponding 30-m Landsat pixel.

used in studies examining the distribution of the fungus *Entomophaga maimaiga* (Elkinton and others 2019), spongy moth outbreaks (Pasquarella and others 2021), runoff (Smith-Tripp and others 2021), nonstructural carbohydrates and mortality (Barker Plotkin and others 2021), and soil nitrogen dynamics (Conrad-Rooney and others 2020). To place our moving-window ensemble results in the context of previous implementations, we compared results generated using this new version of the workflow with three different assessments using the following fixed time period baselines: 2000–2010 and 2005–2015 from the baseline comparison study (Pasquarella and others 2021) and 2000–2010 from the 2018 southern New England reanalysis study (Pasquarella and others 2018). We extracted condition scores from each of these assessments for a set of 486 plots sampled from six 350-ha "hot spots" representing a range of forest types and defoliation severity in the Quabbin Reservoir Watershed in central Massachusetts. These plots generally experienced little if any defoliation during the 2016 spongy moth outbreak event with more significant impacts in 2017 and were surveyed in late summer/early fall of 2017 to characterize post-defoliation canopy recovery (see MacLean and others 2021 for details).

We used a series of scatterplots of results for the years 2016 and 2017 to compare scores generated using different baseline periods and workflows (fig. 9.2). We found that scores for the year 2016 generated using a fixed 2005–2015 baseline were most strongly correlated with those generated using our new approach that used baseline models fit to data from 5-year moving windows across 2005–2015 ($R^2 = 0.91$). The HCM-generated vegetation condition scores were less comparable across older baseline periods, with 2016 results calculated using 2000–2010 baselines showing weaker correlation with the 2016 HCM results calculated using moving-window models fit to the 10 years prior, with R^2 values ranging from 0.62 to 0.70.

As expected, 2017 scores for these sites were generally more negative, reflecting more widespread and significant defoliation. Again, vegetation condition scores generated using the 2005–2015 fixed baseline were most strongly correlated with the HCM approach ($R^2 = 0.80$), where models would be fit to observations from 2006–2016 to generate 2017 results, and less correlated with scores generated using older 2000–2010 baselines ($R^2 = 0.30$ and 0.29). In both years, results from the reanalysis products appear somewhat less correlated with HCM results than the Google Earth Engine implementation for the same baseline period. The results of these exploratory comparisons are in line with previous findings that selection of a baseline period has notable effects on condition score values (Pasquarella and others 2021).

Comparisons with Forest Inventory and Analysis Plot Data/Mortality

We also use our HCM results to investigate relationships between estimated defoliation and tree mortality and growth in FIA plots in Pennsylvania. Morin and Liebhold (2016) found increases in spongy moth host-tree mortality rates and decreases in growth rates in areas where

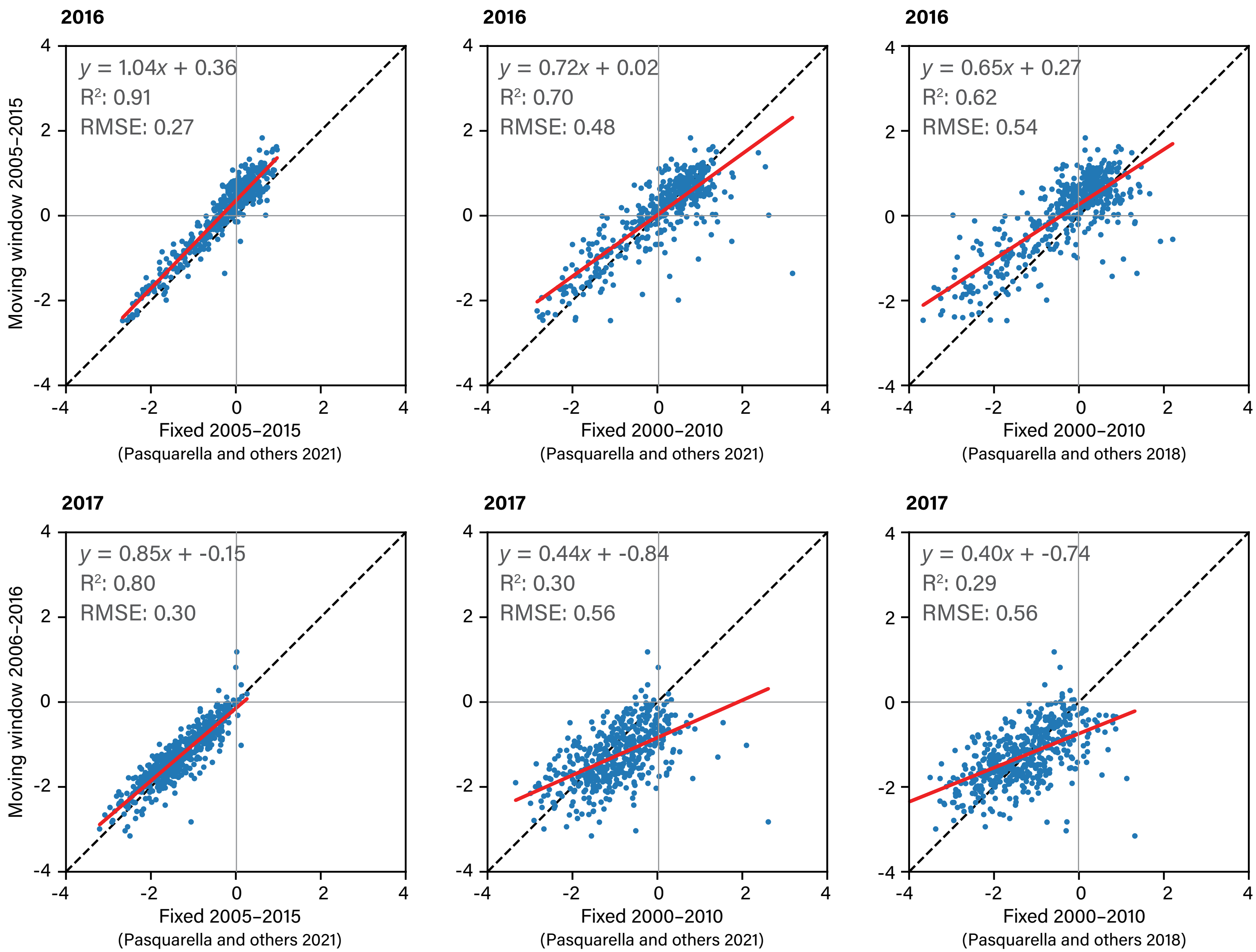

Figure 9.2—Comparison of results for 486 plots sampled from six clusters of plots (hot spots) across the Quabbin Reservoir Watershed in central Massachusetts for the years 2016 and 2017. Condition monitoring scores based on a new moving-window approach are compared with results from previous studies using fixed harmonic baselines, specifically 2005–2015 (left) and 2000–2010 (center) baselines from the baseline comparison study (Pasquarella and others 2021) and the southern New England reanalysis product (right) (Pasquarella and others 2018), which is analogous to the 2000–2010 results generated using Google Earth Engine. All baseline models are fit using Tasseled Cap Greenness using annual and 4-month harmonics and all available Landsat 5, 7, and 8 observations.

multiple years of repeated defoliation within the previous 10 years were observed through aerial sketch-mapping surveys. We conducted a similar analysis using vegetation condition scores from the newly developed procedure in place of sketch-map survey data.

Given FIA plot data must be processed locally, we exported series of annual condition score rasters for our Pennsylvania study area from Google Earth Engine. Although the condition monitoring tool displays assessments for a monitoring period of May through September (05-01 to 10-01), we also tested a more constrained period of June through August (06-01 to 09-01) to better correspond to the expected timing of peak spongy moth defoliation. To account for spatial coherence in defoliated patches and reduce any high-frequency noise, we applied a 3- x 3-pixel (90- x 90-m) smoothing kernel to our outputs.

Following Morin and Liebhold (2016), we used Pennsylvania FIA plots remeasured during 2007–2011 (n = 1,186). For each plot, the minimum vegetation condition score from the 5 years previous to an FIA remeasurement was extracted from the smoothed vegetation condition score rasters (i.e., for an FIA plot measured in 2007, the minimum vegetation condition score was determined based on assessment results from 2002–2006). We used this minimum condition score over the 5-year period prior to remeasurement as an indicator of the severity of peak defoliation, and we also computed the number of years where condition scores fell below a given threshold, i.e., -1.0 or -2.0, as a basic indicator of the frequency/persistence of vegetation condition changes.

We estimated plot-level mortality, growth, growth/volume ratio, and mortality/volume ratio for oak species in plots in the oak-hickory forest type group. We fit general linear models (GLMs) with oak mortality and oak growth as the dependent variables and HCM metrics as independent variables with the models weighted by live oak volume. Both mortality and growth models trended in the expected directions, with mortality increasing for more severe and more frequent disturbances while growth exhibits a decreasing trend (fig. 9.3). Although slope terms were found to be significant for all models (p <0.01), the relationships with HCM-generated vegetation condition scores were quite weak, with R^2 values around 0.01. When relating growth and mortality with frequency of disturbance, i.e., the number of years with scores below -1.0 versus below -2.0, the slopes tended to be greater for the "number of -2 years" metric (fig. 9.4). However, it is important to note that the sample size for plots that intersected pixels with strong decreases in HCM scores was too small to be able to robustly test for differences in mortality and growth across the range of HCM vegetation condition scores, i.e., only 7 plots had 2 or more years <-2 HCM in the 5-year window and 43 plots had 1 year <-2 HCM score.

Although we designed the spatial and temporal scope of this exploratory analysis to match that of Morin and Liebhold (2016), the results suggest a much weaker relationship between defoliation and mortality. This difference is likely due to differences between the aerial sketch-map

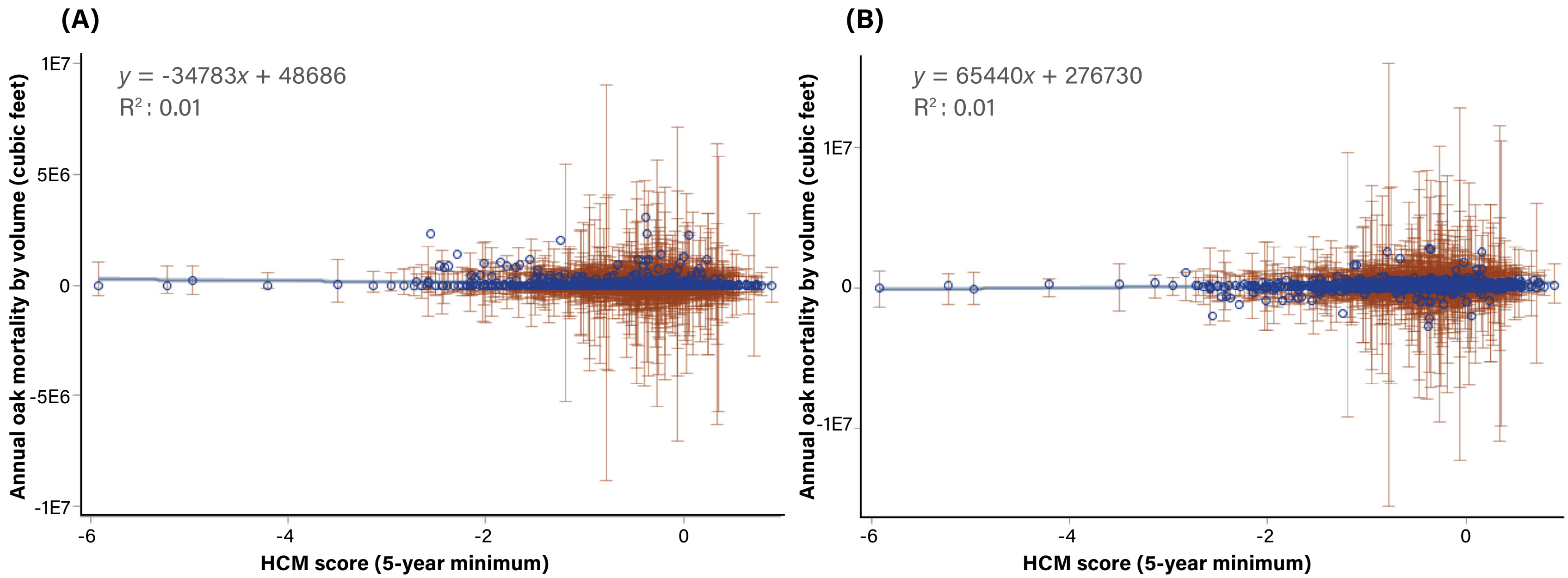

Figure 9.3—(A) Oak mortality and (B) growth by volume as a function of 5-year minimum harmonic condition monitoring (HCM) scores with error bars corresponding to 95-percent prediction limits (weighted). The model suggests mortality is higher and growth is lower for plots with more negative minimum condition scores during the 5-year remeasurement period. Both the slope and intercept terms are significant at p *<0.01; however, the correlations are very weak.*

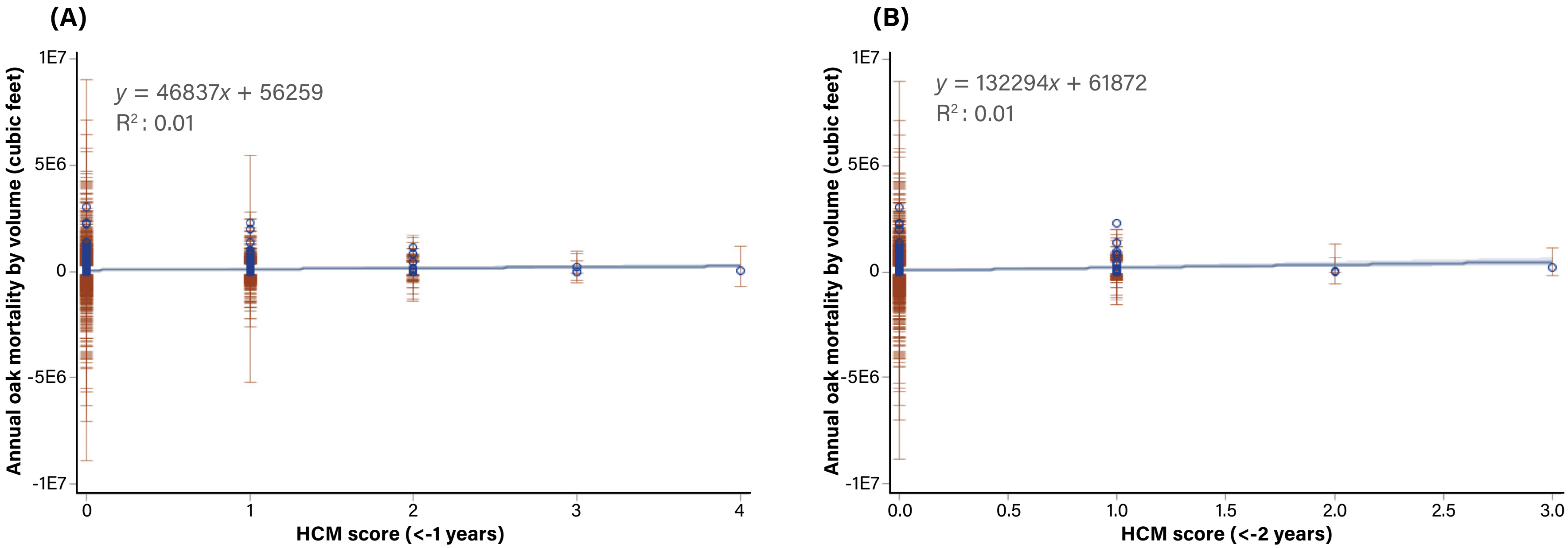

Figure 9.4—Oak mortality by volume as a function of the number of years the 5-year minimum harmonic condition monitoring (HCM) scores fell below -1.0, i.e., showed a Tasseled Cap Greenness (TCG) anomaly two or more times the estimated root mean square error of the (A) baseline models and (B) -2. Error bars correspond to 95-percent prediction limits (weighted). The model suggests increased mortality with increased frequency of anomalously negative HCM scores, and both the slope and intercept terms are significant at p *<0.01; however, the correlations are very weak, and there are relatively few sampled plots that show repeated, high-magnitude changes in TCG.*

polygons used for the original analysis and the HCM-based vegetation condition score rasters used here, which have a finer resolution and increased precision, and are more directly tied to objective measures of change in vegetation greenness. It is also possible that moving-window baselines produce more conservative assessments when multiyear decreases in canopy greenness are included in baseline modeling. Thus, differences observed in this preliminary reanalysis warrant further consideration.

SUMMARY AND CONCLUSIONS

In this project, we introduced an HCM approach that identifies anomalous canopy conditions by fitting a series of harmonic regression models to 5-year moving windows of remotely sensed observations from the Landsat series of satellites rather than relying on a single baseline model derived from a fixed set of years. We share our HCM code as well as an interactive tool for exploring results over a large multistate area (Pasquarella 2021). Our workflow and tool are expected to be a valuable resource for both historic and near-real-time assessments of changes in vegetation condition. Key findings:

- An ensemble of 5-year harmonic baseline models fit using a moving-window approach allows us to characterize the magnitude of spectral change as well as uncertainty in predictions given multiple predictions and dates of observation, and this improved characterization of uncertainty is one of the primary benefits of this approach. This HCM approach is also more flexible than previous fixed-baseline approaches because the baseline period adapts dynamically rather than being specified *a priori*.
- Our comparisons suggest that vegetation condition scores estimated with a moving-window HCM approach are consistent with previous fixed-baseline assessments given the same baseline and monitoring years, though they may diverge more given a greater difference between baseline and monitoring periods. We recommend the moving-window approach for general monitoring over large spatial extents where it would be difficult to prescribe an ideal baseline, although there may be cases where fixing the baseline period to a specific reference period may be preferable, particularly at more localized scales.
- The relationship between vegetation condition scores and mortality of oak in oak/hickory FIA plots in Pennsylvania was difficult to assess based on low numbers of samples that fell into "high disturbance" areas. However, the inconsistency between these results and previous investigations using aerial survey data warrants further consideration, and a larger sample size of impacted plots would be particularly helpful.

It is important to note that the current version of the HCM workflow characterizes spectral anomalies without specific attribution beyond the direction of the change (i.e., an observed area appears more or less green relative to prior years). Future work focusing on combining vegetation condition scores with other spectral inputs and ancillary datasets to differentiate among different types of disturbance, i.e., defoliation, harvest, urban development, is important to consider. There are also opportunities to increase monitoring frequency by extending the Landsat-based approach presented here to other remote sensing instruments and datasets. For example, the Landsat 8 and Sentinel-2 sensors have complementary spectral and spatial resolutions and the combined constellation can provide at least 3- to 4-day revisit time (Li and Roy 2017), and the increased spatial resolution of Sentinel-2 (10- and 20-m bands) could improve detection of finer scale patterns of defoliation and mortality. Differences in estimates of defoliation location, magnitude, and frequency between aerial surveys and Landsat-based estimates are important to be considered for further investigation in terms of both timing and extent of detections.

For more information:
Valerie Pasquarella
vpasquarella@fas.harvard.edu

ACKNOWLEDGMENTS

We thank Audrey Barker Plotkin and Richard MacLean for providing the Quabbin Reservoir Watershed dataset used in this analysis. We also thank Christopher Brown for assistance implementing the moving-window approach for harmonic condition monitoring in Google Earth Engine. Funding for this project was provided by a grant (18-CA-11420004-293) from the USDA Forest Service, Forest Health Protection, Evaluation Monitoring Program. We would like to acknowledge additional support for this work from the Harvard Forest Long Term Ecological Research (LTER) program (NSF DEB #1832210).

LITERATURE CITED

Barker Plotkin, A.; Blumstein, M.; Laflower, D. [and others]. 2021. Defoliated trees die below a critical threshold of stored carbon. Functional Ecology. 35(10): 2156–2167. https://doi.org/10.1111/1365-2435.13891.

Chastain, R.A.; Fisk, H.; Ellenwood, J.R. [and others]. 2015. Near-real time delivery of MODIS-based information on forest disturbances. In: Lippitt, C.D.; Stow, D.A.; Coulter, L.L., eds. Time-sensitive remote sensing. New York: Springer: 147–164. https://doi.org/10.1007/978-1-4939-2602-2_10.

Cohen, W.B.; Healey, S.P.; Yang, Z. [and others]. 2017. How similar are forest disturbance maps derived from different Landsat time series algorithms? Forests. 8(4): 98. https://doi.org/10.3390/f8040098.

Cohen, W.B.; Yang, Z.; Stehman, S.V. [and others]. 2016. Forest disturbance across the conterminous United States from 1985–2012: the emerging dominance of forest decline. Forest Ecology and Management. 360: 242–252. https://doi.org/10.1016/j.foreco.2015.10.042.

Coleman, T.W.; Graves, A.D.; Heath, Z. [and others]. 2018. Accuracy of aerial detection surveys for mapping insect and disease disturbances in the United States. Forest Ecology and Management. 430: 321–336. https://doi.org/10.1016/j.foreco.2018.08.020.

Conrad-Rooney, E.; Barker Plotkin, A.; Pasquarella, V.J. [and others]. 2020. Defoliation severity is positively related to soil solution nitrogen availability and negatively related to soil nitrogen concentrations following a multi-year invasive insect irruption. AoB Plants. 12(6): laa059. https://doi.org/10.1093/aobpla/plaa059.

Crist, E.P. 1985. A TM tasseled cap equivalent transformation for reflectance factor data. Remote Sensing of Environment. 17(3): 301–306. https://doi.org/10.1016/0034-4257(85)90102-6.

Crist, E.R.; Kauth, R.J. 1986. The tasseled cap de-mystified. Photogrammetric Engineering and Remote Sensing. 52: 81–86.

Elkinton, J.S.; Bittner, T.D.; Pasquarella, V.J. [and others]. 2019. Relating aerial deposition of *Entomophaga maimaiga* conidia (Zoopagomycota: Entomophthorales) to mortality of gypsy moth (Lepidoptera: Erebidae) larvae and nearby defoliation. Environmental Entomology. 48(5): 1214–1222. https://doi.org/10.1093/ee/nvz091.

Hall, R.J.; Skakun, R.S.; Arsenault, E.J. 2007. Remotely sensed data in the mapping of insect defoliation. In: Wulder, M.A.; Franklin, S.E., eds. Understanding forest disturbance and spatial pattern; remote sensing and GIS approaches. Boca Raton, FL: CRC Taylor & Francis: 85–111. https://doi.org/10.1201/9781420005189.ch4.

Koltunov, A.; Ramirez, C.M.; Ustin, S.L. [and others]. 2020. eDaRT: the ecosystem Disturbance and Recovery Tracker system for monitoring landscape disturbances and their cumulative effects. Remote Sensing of Environment. 238: 111482. https://doi.org/10.1016/j.rse.2019.111482.

Li, J.; Roy, D.P. 2017. A global analysis of Sentinel-2A, Sentinel-2B and Landsat-8 data revisit intervals and implications for terrestrial monitoring. Remote Sensing. 9(9): 902. https://doi.org/10.3390/rs9090902.

Lister, A.J.; Andersen, H.; Frescino, T. [and others]. 2020. Use of remote sensing data to improve the efficiency of national forest inventories: a case study from the United States national forest inventory. Forests. 11(12): 1364. https://doi.org/10.3390/f11121364.

Lovett, G.M.; Canham, C.D.; Arthur, M.A. [and others]. 2006. Forest ecosystem responses to exotic pests and pathogens in eastern North America. BioScience. 56(5): 395–405. https://doi.org/10.1641/0006-3568(2006)056[0395:FERTEP]2.0.CO;2.

MacLean, R.; Pasquarella, V.; Barker Plotkin, A. 2021. Gypsy moth defoliation survey at the Quabbin Watershed in central Massachusetts 2017. Harvard Forest Data Archive: HF352 (v.3). Environmental Data Initiative. https://doi.org/10.6073/pasta/db7489f4d0e8b00b7c9066aaab554982.

Morin, R.S.; Liebhold, A.M. 2016. Invasive forest defoliator contributes to the impending downward trend of oak dominance in eastern North America. Forestry. 89(3): 284–289. https://doi.org/10.1093/forestry/cpv053.

Norman, S.P.; Christie, W.M. 2020. Satellite-based evidence of forest stress and decline across the conterminous United States for 2016, 2017, and 2018. In: Potter, K.M.; Conkling, B.L., eds. Forest Health Monitoring: national status, trends, and analysis 2019. Gen. Tech. Rep. SRS-250. Asheville, NC: U.S. Department of Agriculture, Forest Service, Southern Research Station: 151–166.

Norman, S.P.; Hargrove, W.W.; Spruce, J.P. [and others]. 2013. Highlights of satellite-based forest change recognition and tracking using the ForWarn system. Gen. Tech. Rep. SRS-180. Asheville, NC: U.S. Department of Agriculture, Forest Service, Southern Research Station. 30 p. https://doi.org/10.2737/SRS-GTR-180.

Pasquarella, V. 2021. Valpasq/condition_monitoring: v0.2-alpha (v0.2-alpha). Zenodo. https://doi.org/10.5281/zenodo.4565535.

Pasquarella, V.J.; Bradley, B.A.; Woodcock, C.E. 2017. Near-real-time monitoring of insect defoliation using Landsat time series. Forests. 8(8): 275. https://doi.org/10.3390/f8080275.

Pasquarella, V.J.; Elkinton, J.S.; Bradley, B.A. 2018. Extensive gypsy moth defoliation in southern New England characterized using Landsat satellite observations. Biological Invasions. 20(11): 3047–3053. https://doi.org/10.1007/s10530-018-1778-0.

Pasquarella, V.J.; Holden, C.E.; Kaufman, L.; Woodcock, C.E. 2016. From imagery to ecology: leveraging time series of all available Landsat observations to map and monitor ecosystem state and dynamics. Remote Sensing in Ecology and Conservation. 2(3): 152–170. https://doi.org/10.1002/rse2.24.

Pasquarella, V.J.; Mickley, J.G.; Barker Plotkin, A. [and others]. 2021. Predicting defoliator abundance and defoliation measurements using Landsat-based condition scores. Remote Sensing in Ecology and Conservation. 7(4): 592–609. https://doi.org/10.1002/rse2.211.

Rullan-Silva, C.D.; Olthoff, A.E.; de la Mata, J.A.D.; Pajares-Alonso, J.A. 2013. Remote monitoring of forest insect defoliation. A review. Forest Systems. 22(3): 377–391. https://doi.org/10.5424/fs/2013223-04417.

Schroeder, T.A.; Healey, S.P.; Moisen, G.G. [and others]. 2014. Improving estimates of forest disturbance by combining observations from Landsat time series with U.S. Forest Service Forest Inventory and Analysis data. Remote Sensing of Environment. 154: 61–73. https://doi.org/10.1016/j.rse.2014.08.005.

Sellers, P.J.; Tucker, C.J.; James Collatz, G. [and others]. 1996. A revised land surface parameterization (SiB2) for atmospheric GCMS. Part II: the generation of global fields of terrestrial biophysical parameters from satellite data. Journal of Climate. 9(4): 706–737. https://doi.org/10.1175/1520-0442(1996)009<0706:ARLSPF>2.0.CO;2.

Senf, C.; Seidel, R.; Hostert, P. 2017. Remote sensing of forest insect disturbances: current state and future directions. International Journal of Applied Earth Observation and Geoinformation. 60: 49–60. https://doi.org/10.1016/j.jag.2017.04.004.

Smith-Tripp, S.; Griffith, A.; Pasquarella, V.J.; Matthes, J.H. 2021. Impacts of a regional multiyear insect defoliation event on growing-season runoff ratios and instantaneous streamflow characteristics. Ecohydrology. 14(7): e2332. https://doi.org/10.1002/eco.2332.

Vogt, J.T.; Koch, F.H. 2016. The evolving role of Forest Inventory and Analysis data in invasive insect research. American Entomologist. 62(1): 46–58. https://doi.org/10.1093/ae/tmv072.

Wilson, B.T. 2015. Harmonic analysis of dense time series of Landsat imagery for modeling change in forest conditions. In: Stanton, S.M.; Christensen, G.A., comps. Pushing boundaries: new directions in inventory techniques and applications: Forest Inventory and Analysis (FIA) symposium 2015. 2015 December 8–10, Portland, OR. Gen. Tech. Rep. PNW-931. Portland, OR: U.S. Department of Agriculture, Forest Service, Pacific Northwest Research Station: 200–205.

Wilson, B.T.; Knight, J.F.; McRoberts, R.E. 2018. Harmonic regression of Landsat time series for modeling attributes from national forest inventory data. ISPRS Journal of Photogrammetry and Remote Sensing. 137: 29–46. https://doi.org/10.1016/j.isprsjprs.2018.01.006.

Wilson, B.T.; Lister, A.J.; Riemann, R.I. 2012. A nearest-neighbor imputation approach to mapping tree species over large areas using forest inventory plots and moderate resolution raster data. Forest Ecology and Management. 271: 182–198. https://doi.org/10.1016/j.foreco.2012.02.002.

Zhu, Z.; Woodcock, C.E.; Olofsson, P. 2012. Continuous monitoring of forest disturbance using all available Landsat imagery. Remote Sensing of Environment. 122: 75–91. https://doi.org/10.1016/j.rse.2011.10.030.